C. R. Chimie 19 (2016) 1254–1265

Contents lists available at ScienceDirect

Comptes Rendus Chimie

www.sciencedirect.com

Account/Revue

Recent progress in catalytic NO decomposition

Masaaki Haneda [a, *], Hideaki Hamada [b]

[a] Advanced Ceramics Research Center, Nagoya Institute of Technology, 10-6-29 Asahigaoka, Tajimi, Gifu 507-0071, Japan
[b] Interdisciplinary Research Center for Catalytic Chemistry, National Institute of Advanced Industrial Science and Technology, Tsukuba Central 5, 1-1-1 Higashi, Tsukuba, Ibaraki 305-8565, Japan

ARTICLE INFO

Article history:
Received 30 May 2015
Accepted 2 July 2015
Available online 2 March 2016

Keywords:
Direct decomposition
Nitrogen monoxide
Perovskite
Rare earth oxide
Cobalt oxide
Oxide anion vacancy
Surface basicity

ABSTRACT

Recent progress in catalytic direct NO decomposition is overviewed, focusing on metal oxide-based catalysts. Since the discovery of the Cu-ZSM-5 catalyst in the early 1990s, various kinds of catalytic materials such as perovskites, C-type cubic rare earth oxides, and alkaline earth based oxides have been reported to effectively catalyze direct NO decomposition. Although the activities of conventional catalysts are poor in the presence of coexisting O_2 and CO_2, some of the catalysts reviewed in this article possess significant tolerance toward these coexisting gases. The active sites for direct NO decomposition are different depending on the types of metal oxide-based catalysts. In the case of perovskite type oxides, oxide anion vacancies act as catalytically active sites on which NO molecules are adsorbed. C-type cubic rare earth oxides contain oxide anion vacancies with large cavity space, enabling easy access of NO molecules and their subsequent adsorption. Surface basic sites on alkaline earth based oxides participate in NO decomposition as active sites on which NO molecules are adsorbed as NO_2^- species. The reaction mechanisms of direct NO decomposition are also discussed.

1. Introduction

Because nitrogen oxides (NO_x), which are thermally formed by radical chain mechanisms proposed by Zeldovich at high temperatures above 1200 °C [1], emitted from combustion facilities are harmful to human health and the global environment, the removal of NO_x from exhaust gas is necessary. Catalysis plays an important role in reducing NO_x. For example, three-way catalysts (TWCs) have already been practically applied to the purification of exhaust gases emitted from gasoline-powered vehicles. TWCs can simultaneously reduce NO and oxidize CO and hydrocarbons at a theoretical air/fuel (A/F) ratio of around 14.6. Selective catalytic reduction of NO_x using urea or ammonia is a leading technology to reduce NO_x emission from diesel exhaust. In this reaction, NO_x are efficiently reduced by ammonia in the presence of excess O_2.

On the other hand, direct NO decomposition ($2NO \rightarrow N_2 + O_2$), which needs no reductants, is well known as the most desirable reaction for NO_x removal. Since the enthalpy of formation for NO is large and positive, $\Delta H^0_{f(298\ K)} = 90.2$ kJ mol^{-1} [2,3], NO molecules are thermodynamically unstable and can be decomposed into N_2 and O_2. However, despite the thermodynamic instability, direct NO decomposition is a kinetically slow reaction because of its high activation energy (~335 kJ mol^{-1}) [2,3]. Therefore, the use of a catalyst is an effective strategy for NO decomposition to proceed, and the development of highly active catalysts still remains a challenging subject of study for the solution of NO_x problems.

Numerous studies have been performed so far on catalytic NO decomposition, and a wide variety of catalytic materials have been found, such as noble metals, metal oxides, and zeolites [4,5]. In this review article, we

* Corresponding author.
E-mail address: haneda.masaaki@nitech.ac.jp (M. Haneda).

http://dx.doi.org/10.1016/j.crci.2015.07.016
1631-0748/

overview recent progress in catalytic NO decomposition especially focusing on metal oxide-based catalysts.

2. Historical perspective on catalytic NO decomposition

Direct NO decomposition with catalysts has been extensively studied since the first report in the beginning of the 20th century by Jellinek [6], who revealed that precious metals such as platinum and iridium can catalyze NO decomposition at temperatures as low as 670 °C. Research activities reported before the 1980's are summarized in a number of excellent reviews [3–5,7,8].

Most of the early studies were performed focusing on the kinetics of NO decomposition. For instance, Amirnazmi et al. [9] studied NO decomposition over Pt/Al_2O_3, and found that the kinetics follow the equation: $r = N\,k(NO)/[1 + \alpha\,K(O_2)]$, where k is a reaction rate constant, K is an adsorption equilibrium constant, and α is a conversion factor. This equation means that the reaction is a first order with respect to NO and oxygen inhibits the reaction. As for metal oxide catalysts, Winter [10] measured the NO decomposition rates on 40 metal oxides, and proposed that the NO decomposition rate is closely dependent on the rate of the O_2 desorption step. Boreskov [11] also measured the catalytic activities of the 4th-period transition metal oxides for various catalytic reactions including NO decomposition and CH_4 oxidation, and revealed a close correlation between the activity for NO decomposition and that for homonuclear exchange of oxygen isotopes. These findings suggest that an effective strategy for the development of highly active NO decomposition catalysts is to create catalytically active sites effectively promoting the O_2 desorption step.

Under these circumstances, Iwamoto et al. developed highly active copper ion exchanged Y zeolites (Cu–Y) [12], based on the finding that oxygen species adsorbed on Cu^{II} cations exchanged into zeolites can desorb at temperatures as low as 300 °C [13]. They also reported that excessively copper ion exchanged ZSM-5 zeolites (Cu-ZSM5) showed quite high NO decomposition activity in the temperature range of 350–600 °C [14]. According to their further studies [15–17], Cu^+ ions in the zeolite produced at elevated temperatures act as catalytically active sites and NO decomposition proceeds via the formation of $NO^{\delta-}$ or $(NO)_2^{\delta-}$ species on Cu^+ and the reversible redox cycle between Cu^{2+} and Cu^+.

Since the discovery of the Cu-ZSM-5 catalyst, extensive studies have been performed to improve its NO decomposition activity [18–21]. For instance, Pârvulescu at el. [22,23] reported that the addition of Sm into Cu-ZSM-5 promotes the O_2 desorption step along with the stabilization of the Cu^I–O–Cu^{II} redox sites, resulting in the enhancement of NO decomposition activity. Yahiro et al. [24] also investigated the effect of coexisting rare earth elements such as La, Ce, Pr, Nd, Sm, and Gd on the activity of Cu-ZSM-5. Among the rare earth elements, Sm and Gd were found to act as promoters for NO decomposition over Cu-ZSM-5. They attributed the promotional effect to the stabilization of Cu^+ active sites to enhance NO adsorption.

In addition to Cu-ZSM-5 catalysts, metal oxides with weak metal–oxygen bonds, such as cobalt oxide [25–27], oxygen-deficient Sr–Fe oxides [28] and perovskite-type compounds [29–31], have been investigated. Fig. 1 shows a rough comparison of the relative catalytic activities reported so far [32]. It is of interest that the key components for direct NO decomposition are Cu and Co, the combination of which with other components would enhance NO decomposition activity. Although Cu-ZSM-5 is still the most active catalyst as can be seen in Fig. 1, some composite oxides such as perovskite show comparable activity in the high temperature region. Therefore, designing and controlling the catalytically active sites may lead to highly active NO decomposition catalysts because of infinite combinations of metal components for composite mixed oxides. In the next section, recent advances in metal oxide-based NO decomposition catalysts will be overviewed.

3. Advances in metal oxide-based NO decomposition catalysts

Many kinds of metal oxides have been reported to effectively catalyze direct NO decomposition. It is of interest that N_2 and O_2 are always formed at a steady state with an O_2/N_2 ratio of approximately unity. The formation of N_2O is almost negligible in NO decomposition over these metal oxide-based catalysts. Recent advances in four different types of metal oxide-based catalysts will be reviewed.

3.1. Perovskite-type oxides

Perovskite-type materials are the oxides having ABO_3 and/or A_2BO_4 structures shown in Fig. 2, where A is a large cation that is coordinated by twelve O^{2-} ions and B is a small cation located at the center of the octahedron. Perovskite-type oxides show good performance for direct NO decomposition, as reviewed by Zhu and Thomas [33], by Imanaka and Masui [34] and by Royer et al. [35]. Major

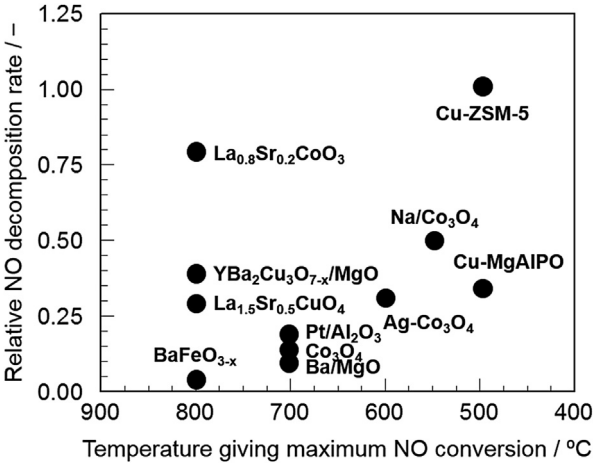

Fig. 1. Comparison of the activity of various catalysts reported so far for direct NO decomposition [32].

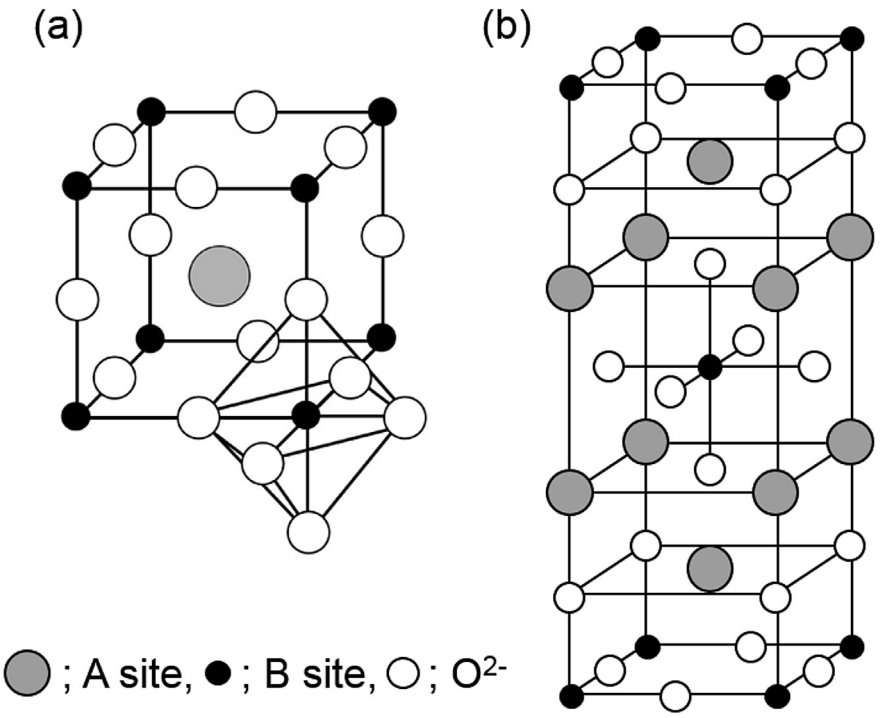

Fig. 2. Crystal structure of (a) ABO_3-type and (b) A_2BO_4-type perovskite oxides [34,48].

reports on perovskite-type oxides are summarized in Table 1.

Since A- and/or B-site cations in the structure are easily replaced by other ions with different ionic sizes and valencies, there are a wide variety of perovskite-type oxides with different elemental combinations. Yokoi and Uchida [36] investigated the influence of transition metals located at the B-site in $LaMO_3$ (M: Cr, Mn, Fe, Co and Ni) on the NO decomposition activity, and found that the activity of $LaMO_3$ was decreased in the order of $LaNiO_3$ > $LaCoO_3$ > $LaMnO_3$ > $LaFeO_3$ > $LaCrO_3$. XPS and molecular orbital calculations suggested that the instability of the

Table 1
Reports on the direct NO decomposition activity of perovskite-type oxides.

Catalyst	NO conversion (%)	Reaction conditions			Ref.
		NO (%)	Temp. (°C)	W/*F* (g s cm^{-3})	
$LaNiO_3$	24	1.0	700	3.0	[36]
$LaSrNiO_4$	93	1.5	900	1.34	[37]
$La_{0.5}Ce_{0.5}SrNiO_4$	70	1.0	800	4.0	[39]
$La_{1.2}Ba_{0.8}NiO_4$	89	4.0	850	1.2	[31]
$LaSrMn_{0.2}Ni_{0.8}O_4$	85	1.0	850	1.2	[40]
$La_{0.87}Sr_{0.13}Mn_{0.2}Ni_{0.8}O_3$	39	2.0	650	4.0	[41]
$SrFe_{0.7}Mg_{0.3}O_3$	86	1.0	950	3.0	[42]
$SrFe_{0.7}Sn_{0.3}O_3$	79	1.0	950	3.0	[42]
$SrFe_{0.7}Zr_{0.3}O_3$	78	1.0	950	3.0	[42]
$SrFe_{0.7}Ni_{0.3}O_3$	76	1.0	950	3.0	[42]
$BaMn_{0.8}Mg_{0.2}O_3$	89	1.0	950	3.0	[43]
$Ba_{0.9}La_{0.1}Mn_{0.8}Mg_{0.2}O_3$	92	1.0	950	3.0	[43]
$SrMn_{0.8}Mg_{0.2}O_3$	78	1.0	950	3.0	[43]
$La_{1.867}Th_{0.1}CuO_{4.005}$	65	0.3	500	7,500 h^{-1} (GHSV)	[44]
$La_{1.6}Th_{0.4}CuO_4$	42	1.0	900	1.33	[45]
La_2CuO_4 nanofiber	100	1.0	300–450	60,000 h^{-1} (GHSV)	[46]
La_2CuO_4 powder	78	1.0	800	60,000 h^{-1} (GHSV)	[46]
$La_{1.5}Sr_{0.5}CuO_4$	40	3.17	800	2.0	[48]
$La_{0.8}Sr_{0.2}CoO_3$	41	3.17	800	2.0	[48]
$Ba_3Y_{3.4}Sc_{0.6}O_9$	91	1.0	950	3.0	[49]
$Sr_{2.7}Ba_{0.3}Fe_{1.8}Zr_{0.2}O_7$	79	1.0	950	3.0	[50]
$La_{0.8}Sr_{0.2}CoO_3$	48	4.0	800	4.0	[84]
$La_{0.4}Sr_{0.6}Mn_{0.8}Ni_{0.2}O_3$	70	4.0	800	4.0	[84]

adsorbed oxygen species, which has weak interactions with the transition metals, is responsible for high NO decomposition activity. Relatively high NO decomposition performances of Ni-substituted perovskite-type oxides such as $LaSrNiO_4$ [37], $La_{1-x}Ce_xSrNiO_4$ ($0 \le x \le 0.3$) [38,39], $La_{2-x}Ba_xNiO_4$ ($x \le 1.2$) [31], $LaSrMn_{1-x}Ni_xO4$ ($0 \le x \le 1$) [40] and $La_{1-x}Sr_xMn_{1-y}Ni_yO_3$ ($0.05 \le x \le 0.6$, $0.6 \le y \le 0.87$) [41] were also reported. Ishihara and co-workers [42,43] studied the effect of B-site substitution on the activity of $SrFe_{0.7}M_{0.3}O_3$ and $BaMn_{0.8}M_{0.2}O_3$ (M: Mg, Si, Ti, Cr, Mn, Fe, Co, Ni, Cu, Ga, Ge, Zr, Ru, Sn, Ce, Ta, and Ir), and found that the substitution with Mg, Zr, Sn, Ni, Co and so on in both catalysts is effective in promoting NO decomposition, while that with Cr and Cu was not effective. They explained the positive effect of B-site substitution with Mg by the acceleration of O_2 desorption.

It was also reported that Cu-substituted perovskite-type oxides such as $La_{2-x}Th_xCuO_4$ ($0 \le x \le 0.4$) [44,45] and La_2CuO_4 [46] show good performance for NO decomposition. For example, Yasuda et al. [30,47,48] extensively studied the effect of the valence state of the Cu site in $La_{2-x}A'_xCu_{1-y}B'_yO_4$, which was controlled by the substitution of A′- and B′-sites with Sr, Ba and Ca, and Zr and Al, respectively, on the NO decomposition activity. They confirmed by XPS that the average oxidation number of Cu varies widely from 1.60 to 2.30 by changing A′- and B′-site elements and their contents. Fig. 3 shows the correlation between the average oxidation number of Cu and the relative catalytic activities at 800 °C, represented by % conversion divided by the surface area. It is of interest that the activities increased sharply with the increase in the average oxidation number of Cu, indicating that controlling the valence state of Cu sites in perovskite-type oxides is one of the effective strategies to develop highly active NO decomposition catalysts.

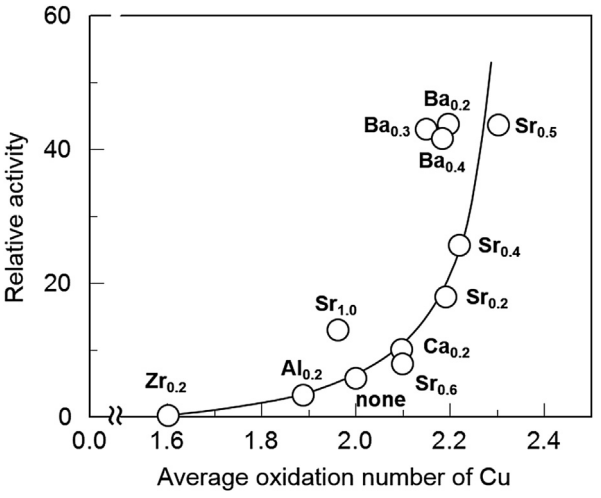

Fig. 3. Change in the NO decomposition activity of $La_{2-x}A'_xCuO_4$ ($A'_x = Zr_{0.2}$, $Al_{0.2}$, $Sr_{0.2}$, $Sr_{0.4}$, $Sr_{0.5}$, $Sr_{0.6}$, $Sr_{1.0}$, $Ba_{0.2}$, $Ba_{0.3}$, $Ba_{0.4}$, $Ca_{0.2}$ and none) at 800 °C and average oxidation number of Cu without pretreatment of the catalyst [30,48]. Reaction conditions: NO = 3.17%, He balance, and $W/F = 2.0$ g s cm^{-3}.

According to the reports by Yasuda et al. [47,48], cations located at the A-sites contribute indirectly to NO decomposition by affecting the electric state of the B-site cations. In other words, transition metals such as Ni, Cu, and Co located at the B-sites are the catalytically active sites for NO decomposition. On the other hand, Goto and Ishihara [49,50] reported that $Ba_3Y_{3.4}Sc_{0.6}O_9$ with a perovskite-related structure, consisting of alkaline earth and rare earth ions, shows high NO decomposition activity in a wide temperature range of 600–850 °C. They also revealed that the addition of BaO into BaY_2O_4 caused a significant increase in the NO decomposition activity [51]. It should be noted that both catalysts do not contain transition metals as catalytically active sites, and that there are no detectable oxide ion vacancies in the BaO/BaY_2O_4 catalyst, although $Ba_3Y_{3.4}Sc_{0.6}O_9$ includes intrinsic oxygen defects in the structure. Therefore, the mechanism of NO decomposition on $Ba_3Y_{3.4}Sc_{0.6}O_9$ and Ba/BaY_2O_4 seems to be different from that on conventional perovskite-type oxide catalysts.

3.2. Rare earth-based oxides

As described above, one of the strategies to develop highly active perovskite-type oxide catalysts for NO decomposition is to control the valence state of the active site for promotion of O_2 desorption. In addition, the creation of oxide anion vacancies would also be effective to promote the dissociation of NO molecules. Non-stoichiometric rare earth oxides such as CeO_2, Pr_6O_{11}, and Tb_4O_7 produce oxygen defects easily on their surface by suitable reduction treatment because the metal valency can change between +3 and +4 depending on the environment [52]. This leads us to the consideration that NO is effectively decomposed on the surface of the non-stoichiometric rare earth oxides. In fact, Daturi et al. [53] observed continuous formation of N_2 when several pulses of NO were introduced to pre-reduced CeO_2–ZrO_2 at 500 °C, indicating that oxide anion vacancies are highly reactive toward NO molecules. Haneda et al. [54] also investigated the surface reactivity of pre-reduced several rare earth oxides with NO molecules, and found that NO was decomposed to N_2 at 400 °C on CeO_2 and Pr_6O_{11} pre-reduced at 500 °C, in which a lot of oxide anion vacancies exist (Table 2). As expected, NO decomposition was not observed over pre-reduced La_2O_3

Table 2
Physical properties and N_2 yield in NO decomposition over rare earth oxides at 400 °C [54].

Catalyst	BET surface area (m^2 g^{-1})	Amount of H_2 consumption below 500 °C in H_2-TPR (μmol $-H_2$ g^{-1})	N_2 yield in NO decomposition[a] (μmol $-N_2$ g^{-1})
La_2O_3	7.5	2.5	0.0
CeO_2	55	75	14.7
Pr_6O_{11}	9.5	773	19.6
Sm_2O_3	8.0	1.5	0.0
Tb_4O_7	22	1008	0.0

Prior to the NO decomposition, the sample was pre-reduced in flowing H_2 at 500 °C for 1 h.

[a] Reaction conditions: NO = 970 ppm, weight = 0.1 g, and gas flow rate = 60 cm^3 min^{-1}.

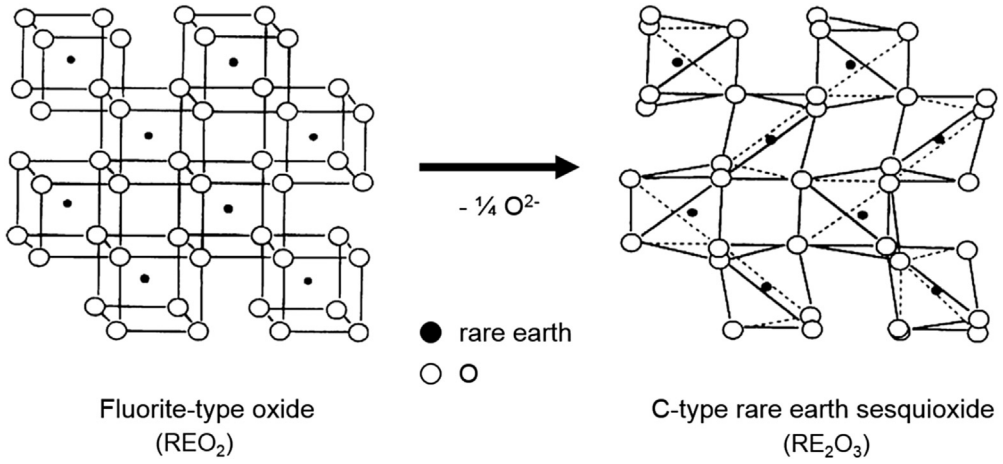

Fig. 4. The relationship between the cubic fluorite-type oxide (REO_2; RE: rare earths) and the C-type rare earth sesquioxide (RE_2O_3) [34,55].

and Sm_2O_3 because oxide anion vacancies are not created in these oxides even after high temperature reduction. Surprisingly, the pre-reduced Tb_4O_7 did not show activity for NO decomposition, although Tb_4O_7 gave the largest amount of H_2 consumption below 500 °C in H_2-TPR, suggesting that the oxide anion vacancy in Tb_4O_7 is not active for the dissociation of NO molecules. NO decomposition on non-stoichiometric rare earth oxides (REO_2, RE: rare earths) may proceed via the following reactions:

$$REO_2 + xH_2 \rightarrow REO_{2-x} + x\text{“}\square\text{”} + xH_2O \quad (1)$$

$$NO + \text{“}\square\text{”} \rightarrow 1/2N_2 + O_{(s)} \quad (2)$$

where “□” and $O_{(s)}$ represent oxygen anion vacancies and surface/subsurface oxygen, respectively. Therefore, the NO decomposition activity must be directly related to the amount of oxide anion vacancies. However, it should be noted that this NO decomposition is not catalytic because oxygen migrated into the oxide anion vacancies cannot be desorbed.

Imanaka et al. [34,55] investigated the catalytic performance of rare earth sesquioxides (RE_2O_3) by focusing on the crystal structure. They speculated that the size of the cavity space of the oxides is an important factor for the NO decomposition activity, because of the improvement of NO accessibility and O_2 desorption. There are three types of crystal structures in the polymorphism of the rare earth sesquioxides, namely, A-type (hexagonal), B-type (monoclinic), and C-type (cubic), according to the ionic size of the rare earth elements [34,55,56]. Among them, the C-type structure possesses the largest cavity space, because it is equivalent to a double edge-sharing fluorite structure (REO_2) with one-quarter of the oxygen sites vacant and with regular ordering, as can be seen in Fig. 4. In other words, the C-type cubic rare earth oxides include many oxide anion vacancies with large cavity space, which may increase the accessibility of NO molecules and their adsorption.

Imanaka and co-workers then studied the catalytic performance of C-type cubic rare earth oxides and reported various kinds of effective composite metal oxides with C-type structures such as Gd_2O_3–Y_2O_3–BaO [57], Yb_2O_3–Tb_4O_7 [58], Y_2O_3–ZrO_2–BaO [59,60], Y_2O_3–Tb_4O_7–BaO [61,62], Y_2O_3–Pr_6O_{11}–Eu_2O_3 [63,64] and Ho_2O_3–ZrO_2–Pr_6O_{11} [65]. As summarized in Table 3, C-type cubic rare earth oxides are highly active catalysts at high temperatures above 800 °C. Among the catalysts reported so far, $(Y_{0.69}Tb_{0.30}Ba_{0.01})_2O_{2.99+\delta}$ was found to be the best catalyst with 100% NO

Table 3
Reports on the direct NO decomposition activity of C-type cubic rare earth oxides.

Catalyst	NO conversion to N_2 (%)	Reaction conditions			Ref.
		NO (%)	Temp. (°C)	W/F (g s cm^{-3})	
$(Gd_{0.70}Y_{0.26}Ba_{0.04})_2O_{2.92}$	75	1.0	900	3.0	[57]
$(Yb_{0.5}Tb_{0.5})_2O_{3\pm\delta}$	55	1.0	900	3.0	[58]
$(Y_{0.94}Zr_{0.06})_2O_{3.06}$	45	1.0	1000	0.375	[59]
$(Y_{0.89}Zr_{0.07}Ba_{0.04})_2O_{3.03}$	90	1.0	900	3.0	[60]
$(Y_{0.70}Tb_{0.30})_2O_{3\pm\delta}$	62	1.0	900	3.0	[62]
$(Y_{0.99}Ba_{0.31})_2O_{3\pm\delta}$	76	1.0	900	3.0	[62]
$(Y_{0.69}Tb_{0.3}Ba_{0.01})_2O_{2.99\pm\delta}$	100	1.0	900	3.0	[61]
$(Y_{0.90}Pr_{0.10})_2O_{3\pm\delta}$	79	1.0	900	3.0	[63]
$(Y_{0.78}Pr_{0.15}Eu_{0.07})_2O_{3\pm\delta}$	84	1.0	900	3.0	[64]
$(Ho_{0.87}Zr_{0.05}Pr_{0.08})_2O_{3.05\pm\delta}$	71	1.0	900	3.0	[65]

conversion at 900 °C (Fig. 5) [55]. The high activity was ascribed to the accelerated oxygen desorption via the redox cycle of Tb^{3+}/Tb^{4+}. In addition, on the basis of mechanistic studies using TPD and in situ FT-IR techniques, the partial substitution of Tb^{3+} sites with Ba^{2+} increases the number of basic sites, thus facilitating NO adsorption, and the generation of oxide anion vacancies in the lattice [62]. They proposed a reaction mechanism in which NO adsorbed as nitrosyl on Ba^{2+} sites reacts with gas-phase NO to form N_2 and O_2, which is then desorbed to the gas-phase via the redox cycle of Tb^{3+}/Tb^{4+}. Thus, the specific structure promoting NO adsorption and oxygen desorption would be one of the important factors for the development of highly active NO decomposition catalysts.

3.3. Alkali or alkaline earth metal-doped cobalt oxide

According to the early work by Boreskov[11], Winter [10], Hightower et al. [7] and Shelef et al. [4,25], cobalt oxide (Co_3O_4) is regarded as one of the most active single metal oxides for NO decomposition. The high activity of Co_3O_4 would be due to the relatively low ΔH of vaporization of O_2 [66]. This means that the Co–O bond strength of Co_3O_4 is relatively weak, making the lattice oxygen to be more easily desorbed. Hamada et al. [26] investigated the additive effect of Ag on the NO decomposition activity of Co_3O_4, based on its weak affinity for oxygen. The addition of a small amount of Ag (Ag/Co atomic ratio = 0.05) was found to significantly increase the catalytic activity of Co_3O_4. On the other hand, Haneda et al. [67,68] reported that pure Co_3O_4 is entirely inactive for direct NO decomposition and that alkali metals remaining as impurities in Co_3O_4 are essential for NO decomposition to occur. Namely, Co_3O_4 prepared by a precipitation method using ammonia, urea, $(NH_4)_2CO_3$ and $(COOH)_2$ as precipitation agents was virtually inactive, whereas Co_3O_4 prepared using Na_2CO_3 effectively catalyzed the NO decomposition reaction. This clearly indicates that the presence of residual Na is important to achieve high NO decomposition activity. This interesting effect of residual Na was first reported by Park et al. [27].

Table 4
BET surface area and activity of alkali-doped Co_3O_4 with an M/Co atomic ratio of 0.035 for direct NO decomposition to N_2 at 600 °C [67].

Catalyst	BET surface area ($m^2\ g^{-1}$)	Activity[a] at 600 °C	
		mol N_2 min^{-1} g^{-1}	mol N_2 min^{-1} m^{-2}
Co_3O_4	9.0	1.35×10^{-8}	1.50×10^{-9}
Li/Co_3O_4	8.3	4.04×10^{-7}	4.87×10^{-8}
Na/Co_3O_4	23	1.72×10^{-6}	6.90×10^{-8}
K/Co_3O_4	34	2.17×10^{-6}	6.39×10^{-8}
Rb/Co_3O_4	38	1.91×10^{-6}	6.60×10^{-8}
Cs/Co_3O_4	33	1.44×10^{-6}	4.38×10^{-8}

NO = 0.1%, He balance, and $W/F = 0.5\ g \cdot s \cdot cm^{-3}$
[a] The reaction rate was determined under the differential conditions obtained at an NO conversion level of below 30%.

Haneda et al. [67,68] studied the additive effect of alkali metals on the activity of Co_3O_4 for NO decomposition. They prepared Co_3O_4 by a precipitation method using urea and then alkali metals (Li, Na, K, Rb, and Cs) were doped into Co_3O_4 by impregnation. As summarized in Table 4, the specific activity of Co_3O_4 at 600 °C, which was calculated by dividing the formation rate of N_2 by the BET surface area, was significantly increased by addition of a small amount of alkali metals (M/Co atomic ratio = 0.035). Fig. 6 shows the dependence of the activities of alkali metal-doped Co_3O_4 on the M/Co atomic ratios at 600 °C. For each catalyst, the activity was increased with the M/Co atomic ratio, and the optimal atomic ratio was at around 0.02–0.05. In addition to alkali metals, promotional effects of alkaline earth metals such as Sr and Ba on the activity of Co_3O_4 was also reported by Haneda et al. [69] and Iwamoto et al. [70]. Since the addition of alkali or alkaline earth metals into Al_2O_3, SiO_2 and ZrO_2 did not generate NO decomposition activity [27,68,70,71], the interaction between Co_3O_4 and alkali or alkaline earth metals must be an essential factor.

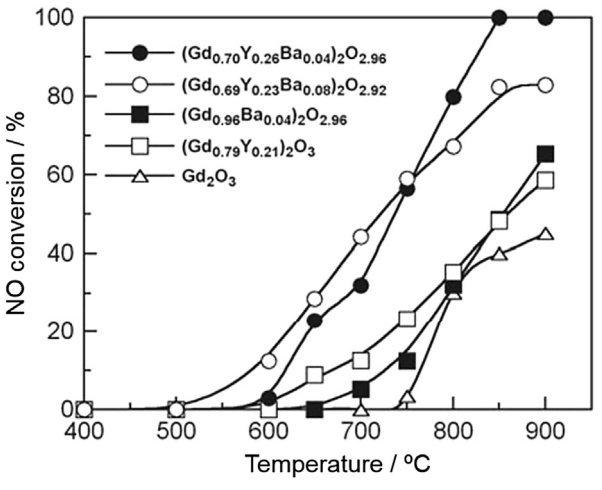

Fig. 5. Temperature dependence of NO conversion on $(Gd_{1-x-y}Y_xBa_y)_2O_{3-y}$ ($0 < x < 0.26$, $0 < y < 0.08$) measured under the conditions of NO = 1% and He balance at $W/F = 0.375\ g\ s\ cm^{-3}$ [55].

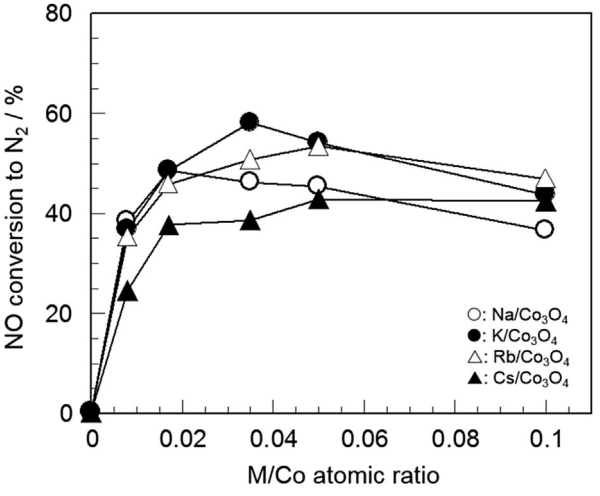

Fig. 6. Change in the NO decomposition activity of alkali-doped Co_3O_4 as a function of the M/Co atomic ratio [67]. Reaction conditions: NO = 0.1%, He balance, and $W/F = 0.5\ g\ s\ cm^{-3}$.

Nakamura et al. [68,72] investigated the role of potassium in NO decomposition over cobalt oxide by a surface science approach. Low energy electron diffraction (LEED) analysis of K-doped CoO/Co(0001) surface suggested that K atoms strongly interact with neighboring Co atoms, leading to a slight reduction of Co atoms to lower oxidation states. A quite similar phenomenon was also reported for K/Co_3O_4 powder catalysts by Haneda et al. [67]. They observed a slight shift of the Co $2p_{3/2}$ binding energy to a lower value in the XPS spectrum when potassium was added to Co_3O_4, indicating a lower valence electronic state of cobalt. The role of alkali metals is probably to weaken the Co–O bond strength, promoting oxygen desorption from Co_3O_4, as shown by the O_2-TPD profiles of alkali metal-doped Co_3O_4 in Fig. 7. Park et al. [27] also reported that the presence of Na facilitated the desorption of oxygen from Co^{3+} to form Co^{2+} via the formation and decomposition of $NaNO_3$ in NO decomposition. On the basis of these reports, it can be concluded that alkali metal additives possess an essential role to create the catalytically active Co^{2+} sites for NO decomposition.

3.4. Barium oxide supported on rare earth oxides

It has been generally accepted that oxide anion vacancies play an important role in direct NO decomposition. Accordingly, extensive studies have been performed to construct oxygen deficient sites in perovskite-type oxides, C-type cubic rare earth oxides and cobalt oxides, as described before. On the other hand, it should be noted that alkaline earth oxides containing no oxygen deficient sites also catalyze NO decomposition [73]. Their activity decreases in the order of BaO > SrO > CaO. In addition, Vannice et al. [74,75] and Xie et al. [76,77] also reported the activity of supported-alkaline earth oxide catalysts such as Sr/La_2O_3, Sr/Sm_2O_3 and Ba/MgO for NO decomposition. They proposed that barium oxide serves as an adsorption site for nitro intermediate species [76]. Because alkaline earth oxides are known to be solid base materials, the basicity of the catalysts seems to be an important factor to determine the NO decomposition activity.

Haneda and co-workers [71] investigated the catalytic performance of supported alkaline earth metal oxides and found that the activity is strongly dependent on the metal oxide support. In Table 5, the NO decomposition activities of supported alkaline earth metal oxides (10.9 wt%) are summarized. As for the supported Ba catalysts, Y_2O_3 is the most effective support. Ba/Y_2O_3 showed the highest NO decomposition activity, which decreased in the order of $Ba/Y_2O_3 > Sr/Y_2O_3 > Ca/Y_2O_3 > Mg/Y_2O_3 > Y_2O_3$. There was no relationship between the BET surface area and NO decomposition activity. They also revealed that the activity of Ba/Y_2O_3 increases with increasing Ba loading up to 5 wt% and that the surface basic sites participate in NO decomposition. These findings suggest that a clarification of the role of surface basic sites is essential for the development of highly active catalysts.

After the report by Haneda and co-workers, many researchers investigated various kinds of Ba catalysts supported on rare earth oxides. For example, Ishihara et al. [51,78] found that BaO catalysts supported on Y_2O_3 and Sc_2O_3 show relatively high NO decomposition activity with an N_2 yield as high as 80% at 950 °C under the conditions of NO = 1% and $W/F = 3.0$ g s cm^{-3}. It was suggested that BaO nano-particles dispersed on the surface of Y_2O_3 and Sc_2O_3 play an important role in NO adsorption. The additive effect of Ba into CeO_2-based mixed oxides such as CeO_x–MnO_x and CeO_x–FeO_x was also reported by Iwamoto et al. [79–83]. They prepared Ba catalysts supported on CeO_x–FeO_x and CeO_x–MnO_x mixed oxides by impregnation

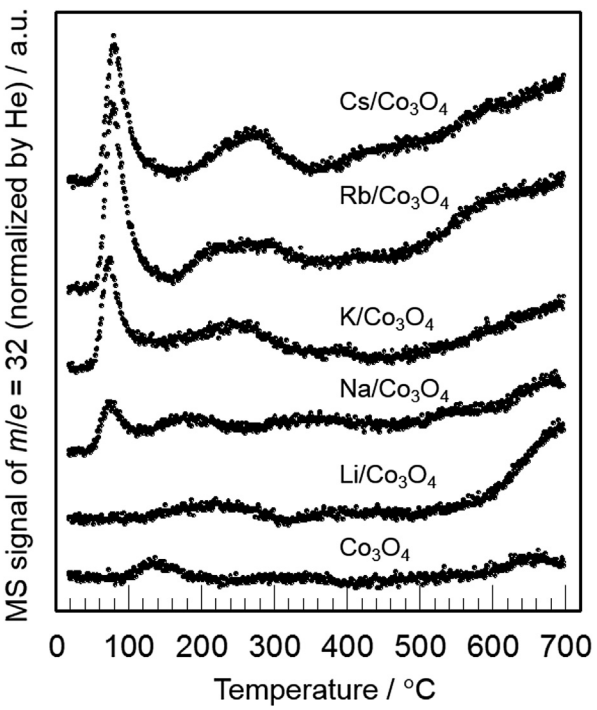

Fig. 7. O_2-TPD profiles of alkali-doped Co_3O_4 with an M/Co atomic ratio of 0.035 [67].

Table 5
BET surface area of and NO conversion on supported alkaline earth metal oxide (10.9 wt%) [71].

Catalyst	BET surface area (m^2 g^{-1})	NO conversion to N_2 (%)		
		700 °C	800 °C	900 °C
Y_2O_3	18.9	2.7	4.7	8.7
MgO	32.0	≤1	≤1	≤1
La_2O_3	7.5	≤1	≤1	3.5
Sm_2O_3	8.0	4.7	10.8	13.9
Al_2O_3	190	≤1	≤1	≤1
SiO_2	286	≤1	≤1	≤1
Ba/Y_2O_3	13.8	4.4	15.7	41.0
Ba/MgO	9.4	8.4	12.2	35.5
Ba/La_2O_3	6.4	≤1	≤1	21.5
Ba/Sm_2O_3	12.8	5.6	14.5	36.1
Ba/Al_2O_3	170	≤1	≤1	≤1
Ba/SiO_2	144	≤1	≤1	≤1
Mg/Y_2O_3		2.2	4.6	7.6
Ca/Y_2O_3		2.8	6.6	15.1
Sr/Y_2O_3	15.9	2.0	3.4	26.4

Reaction conditions: NO = 0.1%, He balance, and $W/F = 0.5$ g s cm^{-3}
"≤1" means that the values are below the identification limit by GC.

combined with glycothermal or solvothermal methods, and measured NO decomposition activity under the conditions of NO = 0.6% and $W/F = 1.0$ g s cm^{-3}. Among the catalysts tested, $Ce_{0.8}Mn_{0.15}Ba_{0.05}O_x$ prepared by a solvothermal method showed the highest activity with an N_2 yield of 77% at 800 °C. On the basis of XRD, Raman and XPS analyses, the additive effect of FeO_x and MnO_x was attributed to the increase in the population of oxygen deficient sites in the CeO_x lattice on which NO dissociation and subsequent O_2 desorption take place. The catalysis of Ba-doped CeO_x–MnO_x and CeO_x–FeO_x seems to be very similar to that of perovskite-type oxides and C-type cubic rare earth oxides as described before.

Haneda et al. performed detailed investigation on the importance of surface basicity of supported-Ba catalysts [84–86]. They prepared Ba-doped rare earth oxides (REOs), which are known to show different surface basicity depending on the radius of the rare earth cations [87], by a coprecipitation method and examined the relationship between NO decomposition activity and surface basicity [85]. Table 6 summarizes the BET surface area and NO decomposition activities of REOs and Ba–REOs evaluated under the conditions of NO = 0.1% and $W/F = 1.0$ g s cm^{-3}. Although REOs without Ba catalyzed NO decomposition, the addition of 8 mol% Ba significantly enhanced the NO decomposition activity. The activity of Ba–REOs was decreased in the order of Ba–Dy_2O_3 ≈ Ba–Sm_2O_3 ≈ Ba–Y_2O_3 > Ba–Nd_2O_3 > Na–Tb_4O_7 > Ba–La_2O_3 >> Ba–Pr_6O_{11} > Ba–CeO_2. Sesquioxides of trivalent rare earth metals such as Y_2O_3 and Dy_2O_3 seem to be effective supports for Ba. No correlation was observed between the BET surface area and catalytic performance for all the catalysts. Fig. 8 shows the relationship between the amount of desorbed CO_2 in the temperature range of 300–600 °C in CO_2-TPD, which corresponds to the amount of Ba species exposed on REO surfaces, and the rate of N_2 formation at 800 °C. It is noteworthy that the N_2 formation rate increases

Table 6
BET surface area and NO decomposition activity of REOs and Ba (8 mol%)–REOs prepared by a coprecipitation method [85].

Catalyst	BET surface area (m^2 g^{-1})	NO conversion to N_2 (%)			
		600 °C	700 °C	800 °C	900 °C
La_2O_3	6.9	0.0	1.1	1.9	2.6
CeO_2	15.2	1.2	1.3	1.4	1.7
Pr_6O_{11}	9.2	1.1	2.0	3.2	4.4
Nd_2O_3	5.0	0.7	1.7	2.1	2.8
Sm_2O_3	9.1	0.9	3.5	9.2	14.6
Gd_2O_3	5.7	0.5	2.6	6.6	11.2
Tb_4O_7	3.6	0.5	3.6	8.7	13.1
Dy_2O_3	9.9	0.7	3.3	6.9	10.5
Y_2O_3	16.6	3.0	8.1	11.8	14.5
Ba–La_2O_3	3.2	0.7	10.4	29.6	43.5
Ba–CeO_2	8.8	1.5	6.7	12.4	14.2
Ba–Pr_6O_{11}	2.7	1.1	8.0	18.0	26.7
Ba–Nd_2O_3	7.1	1.4	14.4	35.9	48.8
Ba–Sm_2O_3	6.0	2.1	17.5	42.8	54.0
Ba–Gd_2O_3	5.3	1.5	13.0	38.2	51.2
Ba–Tb_4O_7	6.1	3.9	15.6	30.9	44.6
Ba–Dy_2O_3	6.7	3.6	19.0	45.1	56.5
Ba–Y_2O_3	14.6	2.8	17.8	40.5	47.6

Reaction conditions: NO = 0.1%, He balance, and $W/F = 1.0$ g s cm^{-3}

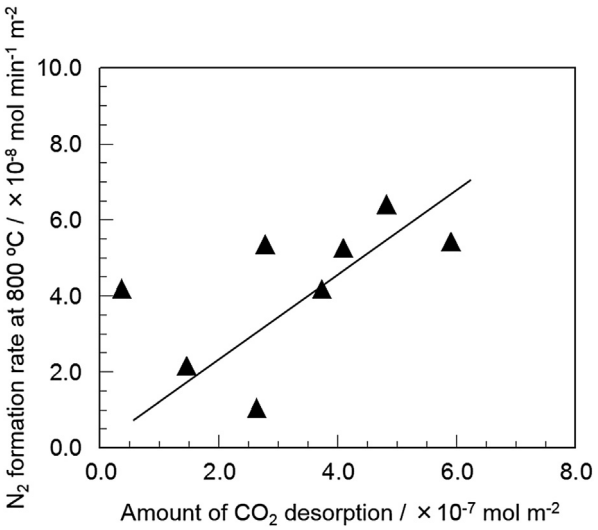

Fig. 8. Relationship between the amount of CO_2 desorption and the rate of N_2 formation at 800 °C over Ba-doped REOs. [85].

with the amount of CO_2 desorption, indicating that the amount of Ba species exposed on REO surfaces determines the NO decomposition activity of Ba-doped REO catalysts.

Haneda et al. also revealed that catalytically inactive $BaCO_3$ is formed when the Ba species was supported on rare earth oxides with strong basic sites, such as La_2O_3 [85]. In other words, the selective formation of catalytically active, highly dispersed Ba species can be expected by controlling the surface basicity of the support oxide. They investigated the additive effect of CeO_2 having weak basicity on the catalytic activity of Ba–Y_2O_3 [86], and found that the addition of CeO_2 decreased the surface basicity of Y_2O_3, resulting in the enhancement of highly dispersed Ba species. In accordance with their assumption, the NO decomposition activity of 8 mol% Ba–Y_2O_3 was improved by the addition of CeO_2 and reached a maximum at a CeO_2 content of 10 mol% (Fig. 9). The predominant role of the CeO_2 additive is not to catalyze NO decomposition but to effectively create the highly dispersed Ba species as catalytically active sites. In contrast to the catalyst materials including oxygen deficient sites such as perovskite-type oxides, Ba-doped REOs are quite unique NO decomposition catalysts, where highly dispersed basic Ba species act as catalytically active sites.

4. Mechanism of NO decomposition on metal oxide catalysts

Kinetic studies of NO decomposition over various catalysts have been extensively performed to reveal the reaction mechanisms. Amirnazmi et al. [9] reported that the kinetics of NO decomposition over Pt/Al_2O_3 and Co_3O_4 catalysts follow the equation: $r = N\ k(NO)/[1 + \alpha K(O_2)]$, suggesting that oxygen inhibition is due to equilibrated chemisorption of oxygen on sites required for the rate-determining process of NO chemisorption. Winter [10] proposed a mechanism in which the reaction is initiated

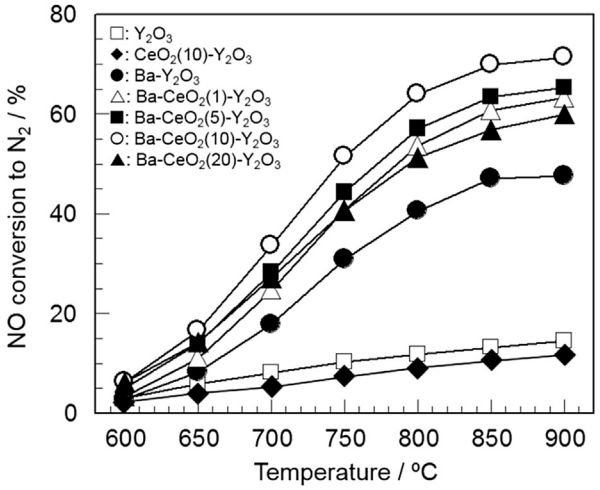

Fig. 9. Activity of Ba (8 mol %) doped CeO_2–Y_2O_3 with various CeO_2 contents for NO decomposition [86]. Reaction conditions: NO = 0.1%, He balance, and $W/F = 1.0$ g s cm^{-3}.

by the attack on NO molecules of surface R_2 centers, which are pairs of adjacent oxygen vacancies with one electron (F^+ centers). A similar reaction mechanism has also been proposed over various metal oxides having oxygen defect sites. For example, Teraoka et al. [88] determined the kinetics of NO decomposition over perovskite-type oxides, and proposed a mechanism in which two NO molecules are adsorbed onto a pair of adjacent oxide ion vacancies as the rate-determining step, followed by desorption of N_2 and O_2. Tsujimoto et al. [62] proposed that direct NO decomposition over C-type cubic rare earth oxides, such as $(Y_{0.69}Tb_{0.30}Ba_{0.01})_2O_{2.99+\delta}$, proceeds via the formation of nitrosyl species on oxide anion vacancies and subsequent reaction with gas-phase NO (Fig. 10).

Vannice et al. [75] suggested a reaction mechanism of NO decomposition over several alkaline earth and rare earth oxides (*e.g.*, La_2O_3 and Sr/La_2O_3) in which oxygen defect sites do not serve as active sites. They proposed a Langmuir–Hinshelwood model in which a quasi-equilibrated NO adsorption step is assumed and a reaction of adsorbed NO leading to the formation of N_2O is the rate-determining step. On the other hand, Xie et al. [76,77] explained NO decomposition over Ba/MgO by a modified Eley–Rideal mechanism, in which the reaction between the gas-phase NO and a surface reactive species, presumably ionic NO*x* species such as NO_2^-, is assumed to be the rate-determining step. As given in Fig. 11, a $Ba^{2+} - NO_2$ species, detected by *in situ* Raman spectroscopy, is proposed to be an intermediate in NO decomposition over Ba/MgO, suggesting that the active sites are not oxygen defects but Ba sites.

Haneda et al. [68,89] investigated the kinetics of NO decomposition over alkali metal-doped Co_3O_4 catalysts, and revealed that NO decomposition proceeds via a bimolecular reaction because the reaction order with respect to NO was higher than unity. The formation of nitrite species (NO_2^-) on the catalyst surface was observed during NO decomposition by *in situ* FT-IR spectroscopy. Isotopic transient kinetic analysis performed by

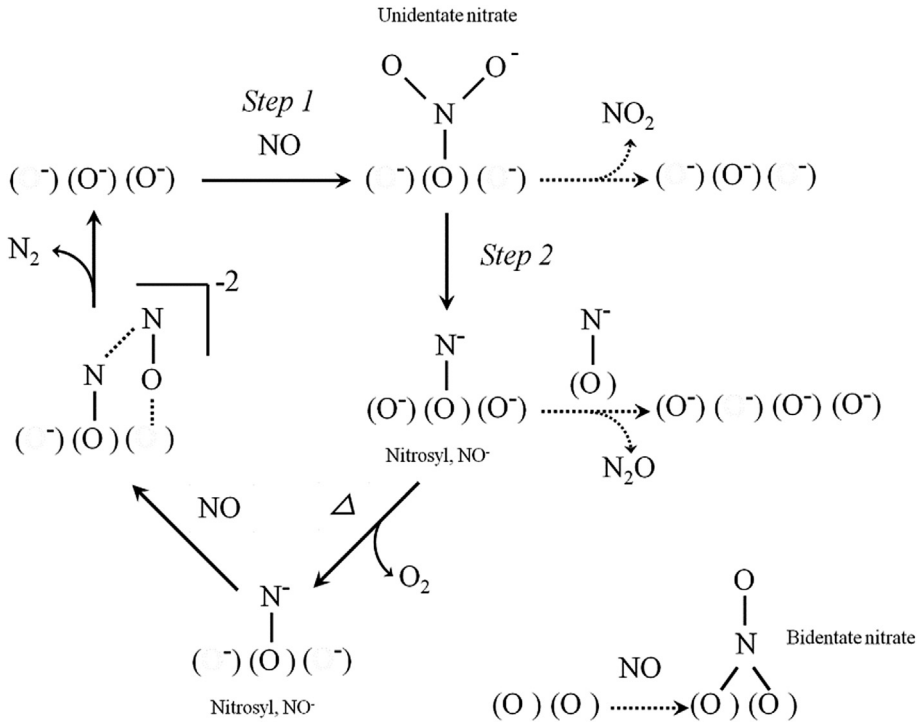

Fig. 10. Proposed mechanism of NO decomposition over C-type cubic rare earth oxides [62].

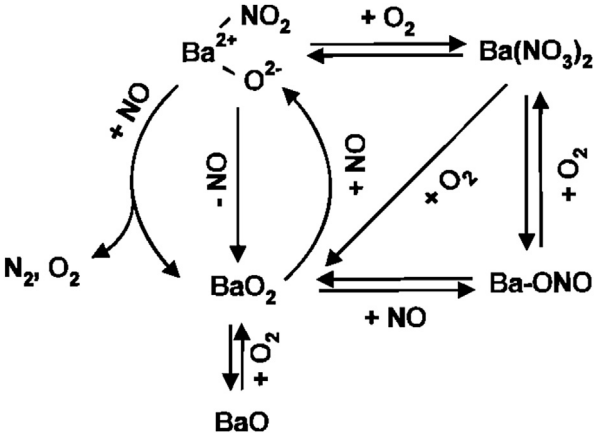

Fig. 11. Proposed reaction scheme of NO decomposition over Ba/MgO [76].

$^{14}NO \rightarrow {}^{15}NO$ switch revealed the formation of mixed labeled $^{14}N^{15}N$ (Fig. 12), suggesting that a surface-adsorbed NO_2^- species serves as an intermediate in the NO decomposition reaction. Because the gas switch from ^{14}NO/He to ^{15}NO/He caused a slow decrease in the formation of $^{14}N_2$, a Langmuir–Hinshelwood model is likely to be a better description of the process. They proposed the following reaction mechanism for NO decomposition over alkali metal-doped Co_3O_4 catalysts:

$$NO(g) + * \rightleftarrows NO* \quad (3)$$

$$NO* + O^{2-} \rightarrow NO_2^-* + [\,]^- \quad (4)$$

$$NO_2^-* + NO* + [\,]^- \not\rightarrow N_2O_x* + O^{2-} + * \ (x < 3) \quad (5)$$

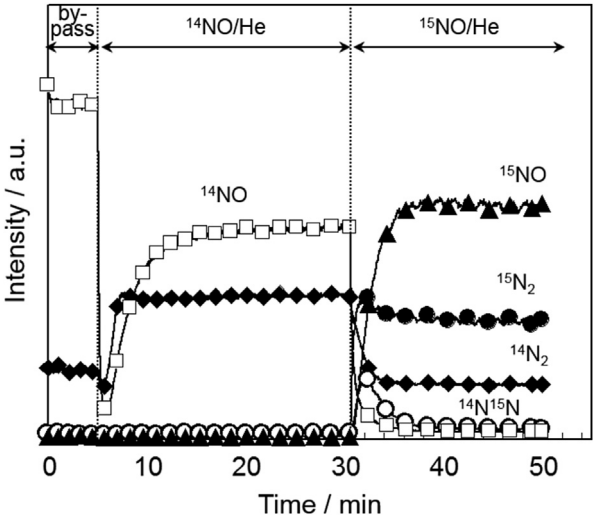

Fig. 12. Product responses ($^{14}N_2$, $^{14}N^{15}N$, $^{15}N_2$, ^{14}NO, and ^{15}NO) following the replacement of ^{14}NO/He with ^{15}NO/He in the reaction stream over K/Co_3O_4 at 600 °C [68,89]. Conditions: NO = 3000 ppm, gas flow rate = 30 $cm^3\ min^{-1}$, and catalyst weight = 0.1 g.

$$N_2O_x* + (x-1)* \rightarrow N_2(g) + xO* \ (x < 3) \quad (6)$$

$$2O* \rightleftarrows O_2(g) + 2* \quad (7)$$

Haneda et al. [84–86] also performed a mechanistic study of NO decomposition over $Ba-Y_2O_3$ and $Ba-CeO_2-Y_2O_3$ catalysts by *in situ* FT-IR spectroscopy and isotopic transient kinetic analysis. In accordance with the reaction over alkali metal-doped Co_3O_4 catalysts, a reaction mechanism was proposed in which NO is adsorbed onto Ba sites as NO_2^- species, which migrates to the interface between Ba and Y_2O_3, and then reacts with the adsorbed NO species to form N_2.

5. Influence of coexisting gases on NO decomposition

Although a wide variety of catalysts have been found for direct NO decomposition as mentioned before, coexisting gaseous O_2 significantly decreases the activity of almost all the NO decomposition catalysts. This is due to the strong adsorption of O_2 on the catalytically active sites, inhibiting NO adsorption. Amirnazmi et al. [9] reported that the reciprocal rate of NO decomposition over Pt/Al_2O_3 is linearly proportional to the O_2 concentration, indicating that the reaction order with respect to O_2 is *ca.* −1.0. Iwamoto et al. [15] examined the influence of coexisting O_2 on the NO decomposition activity of Cu-ZSM-5 with a Cu ion exchange level of 122% under the conditions of NO = 0.5% and $W/F = 4.0$ g s cm^{-3}, and found that the maximum NO conversion was slightly decreased from 55% to 40% when 8% O_2 was added to the reaction gas. On the other hand, they also revealed that the maximum NO conversion over Cu-ZSM-5 was drastically decreased from 23% to 2% by the addition of 1% O_2 into 0.1% NO/He reaction gas. The influence of coexisting O_2 on the NO decomposition activity seems to be dependent on the NO concentration.

Effects of the O_2 concentration on the NO decomposition activity of metal oxide-based catalysts including perovskite-type oxides have also been examined by many researchers. For instance, Ishihara et al. [43,90] investigated the effect of coexisting O_2 on NO decomposition over $BaMnO_3$-based perovskite-type oxides. They revealed that the activity of $La_{0.7}Ba_{0.3}Mn_{0.8}In_{0.2}O_3$ was significantly inhibited by the presence of O_2 with a reaction order of −0.53, while the substitution of Mn sites with Mg ($BaMn_{0.8}Mg_{0.2}O_3$) relieved the inhibiting effect of coexisting O_2 with a reaction order of −0.18. Haneda et al. [86,89] performed a kinetic study on NO decomposition over alkali metal-doped Co_3O_4 and CeO_2-doped $Ba-Y_2O_3$ catalysts and found that the presence of O_2 decreased the NO decomposition activity with reaction orders between −0.26 and −0.40 depending on the types of catalysts. They also compared the catalytic activities of K/Co_3O_4 (K/Co = 0.035), Cu-ZSM-5 (Cu, 3.2 wt%), Pd/Al_2O_3 (Pd, 1 wt%) and $Ba-CeO_2(10)-Y_2O_3$ (Ba, 8 mol%) for direct NO decomposition in the absence and presence of 1% O_2 under the conditions of NO = 0.1% and $W/F = 0.5$ g s cm^{-3} [67,86]. As is presented in Fig. 13, the effective temperatures giving high NO decomposition activity changed depending on the

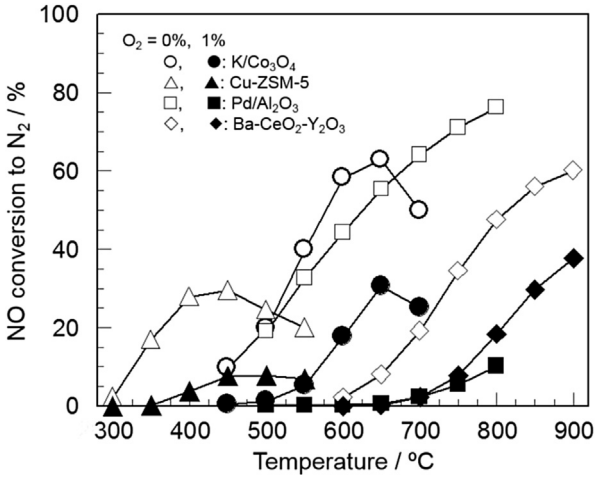

Fig. 13. Comparison of the catalytic activity of K/Co_3O_4 (K/Co = 0.035), Cu-ZSM-5 (Cu, 3.2 wt%), Pd/Al_2O_3 (Pd, 1 wt%) and $Ba–CeO_2(10)–Y_2O_3$ (Ba, 8 mol %) for NO decomposition [67,86]. Conditions: NO = 1000 ppm, O_2 = 0 or 1%, He balance, and $W/F = 0.5$ g s cm^{-3}.

catalysts: 550–700 °C for K/Co_3O_4, 350–550 °C for Cu-ZSM-5, above 650 °C for Pd/Al_2O_3 and above 650 °C for $Ba–CeO_2(10)–Y_2O_3$. The extent of activity depression by O_2 also changed depending on the catalysts; namely, the activity depression of Cu-ZSM-5 and Pd/Al_2O_3 was noticeable, while that of $Ba–CeO_2–Y_2O_3$ and K/Co_3O_4 was not so large. It is noteworthy that the maximum NO conversion on $Ba–CeO_2–Y_2O_3$ was higher than that over Cu-ZSM-5 and K/Co_3O_4.

In addition to O_2, CO_2 is another important constituent which may affect direct NO decomposition because the NO decomposition process would be used for exhaust gas treatment of combustion facilities. Teraoka et al. [91] investigated the effect of CO_2 on NO decomposition over La-based perovskites, using $La_{0.8}Sr_{0.2}CoO_3$ as a representative catalyst sample. The N_2 yield on $La_{0.8}Sr_{0.2}CoO_3$ was drastically decreased from *ca.* 58% to *ca.* 10% by the coexistence of 5% CO_2 under the conditions of NO = 0.9% and $W/F = 4.0$ g s cm^{-3} at 800 °C. It is noteworthy, however, that the NO decomposition activity was almost completely recovered after CO_2 removal from the reaction gas. They considered that the CO_2 impact is related to the formation of carbonate species, which may hinder the access of NO molecules to the catalytically active oxide anion vacancies. Iwakuni et al. [92] also reported that the N_2 yield on the $BaMnO_3$-based perovskite, $Ba_{0.8}La_{0.2}Mn_{0.2}O_3$, decreased from 70% to 30% by the addition of 1% CO_2 into the reaction gas composed of 1% NO/He ($W/F = 3.0$ g s cm^{-3}) at 850 °C, indicating a much larger negative effect than that seen with O_2. The negative effect of CO_2 was even stronger in NO decomposition over the catalysts including alkaline earth elements such as Ba. This is probably because CO_2 strongly adsorbs on alkaline earth metals, forming thermally stable carbonate species.

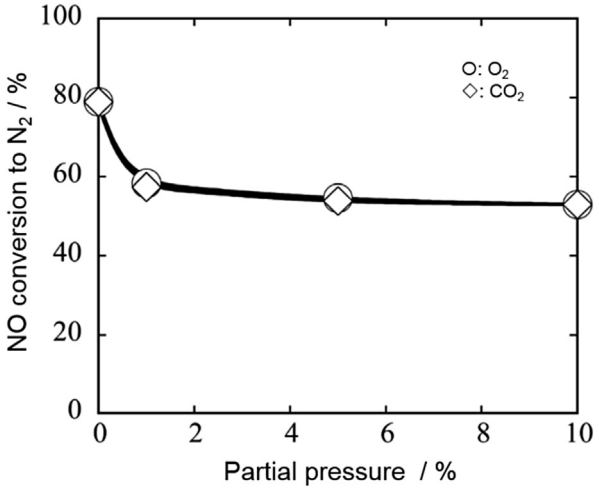

Fig. 14. Effect of partial pressures of O_2 and CO_2 in the feed gas on the conversion of NO over the $(Y_{0.90}Pr_{0.10})_2O_{3+\delta}$ catalyst at 900 °C [63]. Conditions: NO = 1.0%, O_2 = 0–10%, CO_2 = 0–10%, He balance, and $W/F = 3.0$ g s cm^{-3}.

On the other hand, Imanaka et al. [58,63–65] reported relatively high tolerance toward CO_2 for C-type cubic rare earth oxides not including alkaline earth elements. As given in Fig. 14, the N_2 yield on $(Y_{0.90}Pr_{0.10})_2O_{3+\delta}$ was decreased from 80% to 58% by the coexistence of 1% CO_2 under the conditions of NO = 1.0% and $W/F = 3.0$ g s cm^{-3} at 900 °C. However, further increase in the CO_2 concentration up to 10% did not cause significant decreases in the NO decomposition activity [63]. CO_2 poisoning seems to be much smaller for C-type cubic rare earth oxides than that observed for other conventional catalysts such as perovskite-type oxides. Long-term durability tests are necessary to understand the potential of C-type cubic rare earth oxides for practical applications.

6. Conclusions

The direct NO decomposition, which needs no reductants, is the most desirable NO_x abatement technology. Since the discovery of Cu-ZSM-5 as an epoch-making NO decomposition catalyst [5], various kinds of catalysts have been reported to effectively catalyze this reaction. However, no catalysts exhibit high activity under realistic conditions in the presence of coexisting gases (O_2, CO_2, H_2O) and at high space velocities. Recently, various kinds of metal oxide-based catalysts such as perovskites, C-type cubic rare earth oxides and alkaline earth based oxides have been developed as new types of catalysts for possible practical applications, although the NO_x removal performance needs more improvement. Further studies should be continued on the basis of the current knowledge on the structure of catalytically active sites and reaction mechanisms described in this article.

Acknowledgments

This study was partially supported by a Grant–in–Aid for Scientific Research (No. 22350068) from the Ministry of Education, Culture, Sports, Science, and Technology of Japan.

References

[1] Z.R. Ismagilov, M.A. Kerzhentsev, Catal. Rev.—Sci. Eng. 32 (1990) 51.
[2] H. Wise, M.F. Frech, J. Chem. Phys. 20 (1952) 22.
[3] F. Garin, Appl. Catal. A 222 (2001) 183.
[4] M. Shelef, Catal. Rev.—Sci. Eng. 11 (1975) 1.
[5] M. Iwamoto, H. Hamada, Catal. Today 10 (1991) 57.
[6] K. Jellinek, Z. Anorg. Allg. Chem. 49 (1906) 229.
[7] J.W. Hightower, D.A. Van Leirsburg, in: R.M. Klimisch, J.G. Larson (Eds.), The Catalytic Chemistry of Nitrogen Oxides, Plenum Press, London, 1975, pp. p.63–93.
[8] T. Uchijima, Hyomen 18 (1980) 132.
[9] A. Amirnazmi, J.E. Benson, M. Boudart, J. Catal. 30 (1973) 55.
[10] E.R.S. Winter, J. Catal. 22 (1971) 158.
[11] G.K. Boreskov, Discuss. Faraday Soc. 41 (1966) 263.
[12] M. Iwamoto, S. Yokoo, K. Sasaki, S. Kagawa, J. Chem. Soc. Faraday Trans. 1 77 (1981) 1629.
[13] M. Iwamoto, K. Murayama, N. Yamazoe, T. Seiyama, J. Phys. Chem. 81 (1977) 622.
[14] M. Iwamoto, H. Yahiro, K. Tanda, N. Mizuno, Y. Mine, S. Kagawa, J. Phys. Chem. 95 (1991) 3727.
[15] M. Iwamoto, N. Mizuno, H. Yahiro, J. Jpn. Petrol. Inst. 34 (1991) 375.
[16] M. Iwamoto, H. Yahiro, N. Mizuno, W.-X. Zhang, Y. Mine, H. Furukawa, S. Kagawa, J. Phys. Chem. 96 (1992) 9360.
[17] H. Yahiro, M. Iwamoto, Appl. Catal. A 222 (2001) 163.
[18] R. Pirone, P. Ciambelli, G. Moretti, G. Russo, Appl. Catal. B 8 (1996) 197.
[19] V.I. Pârvulescu, P. Grange, B. Delmon, Appl. Catal. B 33 (2001) 223.
[20] M. Yu Kustova, S.B. Rasmussen, A.L. Kustov, C.H. Christensen, Appl. Catal. B 67 (2006) 60.
[21] Y. Shi, H. Pan, Z. Li, Y. Zhang, W. Li, Catal. Commun. 9 (2008) 1356.
[22] V.I. Pârvulescu, P. Oelker, P. Grange, B. Delmon, Appl. Catal. B 16 (1998) 1.
[23] V.I. Pârvulescu, M.A. Centeno, P. Grange, B. Delmon, J. Catal. 191 (2000) 445.
[24] H. Yahiro, T. Nagano, H. Yamaura, Catal. Today 126 (2007) 284.
[25] H.C. Yao, M. Shelef, in: R.M. Klimisch, J.G. Larson (Eds.), The Catalytic Chemistry of Nitrogen Oxides, Plenum Press, London, 1975, pp. p.45–59.
[26] H. Hamada, Y. Kintaichi, M. Sasaki, T. Ito, Chem. Lett. 19 (1990) 1069.
[27] P.W. Park, J.K. Kil, H.H. Kung, M.C. Kung, Catal. Today 42 (1998) 51.
[28] S. Shin, Y. Hatakeyama, K. Ogawa, K. Shimomura, Mater. Res. Bull. 14 (1979) 133.
[29] H. Shimada, S. Miyama, H. Kuroda, Chem. Lett. 17 (1988) 1797.
[30] H. Yasuda, N. Mizuno, M. Misono, J. Chem. Soc., Chem. Commun. (1990) 1094.
[31] Y. Zhu, D. Wang, F. Yuan, G. Zhang, H. Fu, Appl. Catal. B 82 (2008) 255.
[32] M. Iwamoto, Stud. Surf. Sci. Catal. 130 (2000) 23.
[33] J. Zhu, A. Thomas, Appl. Catal. B 92 (2009) 225.
[34] N. Imanaka, T. Masui, Appl. Catal. A 431–432 (2012) 1.
[35] S. Royer, D. Duprez, F. Can, X. Courtois, C.B. Dupeyrat, S. Laassiri, H. Alamdari, Chem. Rev. 114 (2014) 10292.
[36] Y. Yokoi, H. Uchida, Catal. Today 42 (1998) 167.
[37] Z. Zhao, X. Yang, Y. Wu, Appl. Catal. B 8 (1996) 281.
[38] J. Zhu, D. Xiao, J. Li, X. Yang, Y. Wu, J. Mol. Catal. A 234 (2005) 99.
[39] J. Zhu, D. Xiao, J. Li, X. Yang, K. Wei, Catal. Commun. 7 (2006) 432.
[40] J. Zhu, D. Xiao, J. Li, X. Yang, Catal. Lett. 129 (2009) 240.
[41] C. Tafan, D. Klvana, J. Kirchnerova, Appl. Catal. A 223 (2002) 275.
[42] H. Iwakuni, Y. Shinmyou, H. Matsumoto, T. Ishihara, Bull. Chem. Soc. Jpn. 80 (2007) 2039.
[43] H. Iwakuni, Y. Shinmyou, H. Yano, H. Matsumoto, T. Ishihara, Appl. Catal. B 74 (2007) 299.
[44] L.Z. Gao, C.T. Au, Catal. Lett. 65 (2000) 91.
[45] J. Zhu, Z. Zhao, D. Xiao, J. Li, X. Yang, Y. Wu, Catal. Commun. 7 (2006) 29.
[46] L. Gao, H.T. Chua, S. Kawi, J. Solid State Chem. 181 (2008) 2804.
[47] H. Yasuda, T. Nitadori, N. Mizuno, M. Misono, Bull. Chem. Soc. Jpn. 66 (1993) 3492.
[48] H. Yasuda, T. Nitadori, N. Mizuno, M. Misono, Nippon Kagaku Kaishi (1991) 604.
[49] K. Goto, T. Ishihara, Appl. Catal. A 409–410 (2011) 66.
[50] T. Ishihara, Y. Shinmyo, K. Goto, N. Nishiyama, H. Iwakuni, H. Matsumoto, Chem. Lett. 37 (2008) 318.
[51] K. Goto, H. Matsumoto, T. Ishihara, Top. Catal. 52 (2009) 1776.
[52] M.P. Rosynek, Catal. Rev. Sci. Eng. 16 (1977) 111.
[53] M. Daturi, N. Bion, J. Saussey, J.-C. Lavalley, C. Hedouin, T. Seguelong, G. Blanchard, Phys. Chem. Chem. Phys. 3 (2001) 252.
[54] M. Haneda, Y. Kintaichi, H. Hamada, Phys. Chem. Chem. Phys. 4 (2002) 3146.
[55] N. Imanaka, T. Masui, Chem. Rec. 9 (2009) 40.
[56] G. Adachi, N. Imanaka, Chem. Rev. 98 (1998) 1479.
[57] N. Imanaka, T. Masui, H. Masaki, Adv. Mater. 19 (2007) 3660.
[58] S. Tsujimoto, C. Nishimura, T. Masui, N. Imanaka, Chem. Lett. 40 (2011) 708.
[59] H. Masaki, T. Masui, N. Imanaka, J. Alloys. Compd 451 (2008) 406.
[60] S. Tsujimoto, X. Wang, T. Masui, N. Imanaka, Bull. Chem. Soc. Jpn. 84 (2011) 807.
[61] S. Tsujimoto, K. Mima, T. Masui, N. Imanaka, Chem. Lett. 39 (2010) 456.
[62] S. Tsujimoto, K. Yasuda, T. Masui, N. Imanaka, Catal. Sci. Technol. 3 (2013) 1928.
[63] S. Tsujimoto, T. Masui, N. Imanaka, RSC Adv. 4 (2014) 1146.
[64] T. Masui, S. Uejima, S. Tsujimoto, R. Nagai, N. Imanaka, Catal. Today 242 (2015) 338.
[65] S. Tsujimoto, C. Nishimura, T. Masui, N. Imanaka, Catal. Commun. 43 (2014) 84.
[66] B.A. Sazonov, V.V. Popovskii, G.K. Boreskov, Kinet. Catal. 9 (1968) 255.
[67] M. Haneda, Y. Kintaichi, N. Bion, H. Hamada, Appl. Catal. B 46 (2003) 473.
[68] M. Haneda, I. Nakamura, T. Fujitani, H. Hamada, Catal. Surv. Asia 9 (2005) 207.
[69] M. Haneda, G. Tsuboi, Y. Nagao, Y. Kintaichi, H. Hamada, Catal. Lett. 97 (2004) 145.
[70] S. Iwamoto, R. Takahashi, M. Inoue, Appl. Catal. B 70 (2007) 146.
[71] G. Tsuboi, M. Haneda, Y. Nagao, Y. Kintaichi, H. Hamada, J. Jpn. Petrol. Inst. 48 (2005) 53.
[72] I. Nakamura, M. Haneda, H. Hamada, T. Fujitani, J. Electron Spectrosc. Rel. Phenom 150 (2006) 150.
[73] P.J. Meubus, J. Electrochem. Soc. 124 (1977) 49.
[74] X. Zhang, A.B. Walters, M.A. Vannice, J. Catal. 155 (1995) 290.
[75] M.A. Vannice, A.B. Walters, X. Zhang, J. Catal. 159 (1996) 119.
[76] S. Xie, G. Mestl, M.P. Rosynek, J.H. Lunsford, J. Am. Chem. Soc. 119 (1997) 10186.
[77] S. Xie, M.P. Rosynek, J.H. Lunsford, J. Catal. 188 (1999) 24.
[78] T. Ishihara, K. Goto, Catal. Today 164 (2011) 484.
[79] W.-J. Hong, S. Iwamoto, M. Inoue, Catal. Lett. 135 (2010) 190.
[80] W.-J. Hong, S. Iwamoto, S. Hosokawa, K. Wada, H. Kanai, M. Inoue, J. Catal. 277 (2011) 208.
[81] W.-J. Hong, S. Iwamoto, M. Inoue, Catal. Today 164 (2011) 489.
[82] W.-J. Hong, M. Ueda, S. Iwamoto, S. Hosokawa, K. Wada, H. Kanai, H. Deguchi, M. Inoue, Appl. Catal. B 106 (2011) 142.
[83] W.-J. Hong, M. Ueda, S. Iwamoto, S. Hosokawa, K. Wada, M. Inoue, Catal. Lett. 142 (2012) 32.
[84] M. Haneda, Y. Doi, M. Ozawa, Bull. Chem. Soc. Jpn. 84 (2011) 1383.
[85] Y. Doi, M. Haneda, M. Ozawa, J. Mol. Catal. A 383-384 (2014) 70.
[86] Y. Doi, M. Haneda, M. Ozawa, Bull. Chem. Soc. Jpn. 88 (2015) 117.
[87] S. Sato, R. Takahashi, M. Kobune, H. Gotoh, Appl. Catal. A 356 (2009) 57.
[88] Y. Teraoka, T. Harada, S. Kagawa, J. Chem. Soc. Faraday Trans. 94 (1998) 1887.
[89] M. Haneda, Y. Kintaichi, H. Hamada, Appl. Catal. B 55 (2005) 169.
[90] T. Ishihara, M. Ando, K. Sada, K. Takiishi, K. Yamada, H. Nishiguchi, Y. Takita, J. Catal. 220 (2003) 104.
[91] Y. Teraoka, K. Torigoshi, S. Kagawa, Bull. Chem. Soc. Jpn. 74 (2001) 1161.
[92] H. Iwakuni, Y. Shinmyou, H. Yano, K. Goto, H. Matsumoto, T. Ishihara, Bull. Chem. Soc. Jpn. 81 (2008) 1175.